From plastic-waste to H2: Electrolysis of a Poly(methyl methacrylate) model molecule on polymer electrolyte membrane reactors

N Grimaldos-Osorio, F Sordello, M Passananti, P. Vernoux, A Caravaca

From plastic-waste to H_2: electrolysis of a Poly(methyl methacrylate) model molecule on polymer electrolyte membrane reactors

N. Grimaldos-Osorio[1, 2], F. Sordello[2], M. Passananti[2], P. Vernoux[1*], A. Caravaca[1*]

[1] Université de Lyon, Institut de Recherches sur la Catalyse et l'Environnement de Lyon, UMR 5256, CNRS, Université Claude Bernard Lyon 1, 2 avenue A. Einstein, 69626 Villeurbanne, France

[2] Dipartimento di Chimica, Universitá di Torino, Via Pietro Giuria 5, 10125 Turin, Italy

Keywords: Hydrogen production, PEM electrolysis cell, plastic-waste valorisation, PMMA valorisation, methyl pivalate model molecule

***Corresponding authors:** angel.caravaca@ircelyon.univ-lyon1.fr

philippe.vernoux@ircelyon.univ-lyon1.fr

Abstract

Hydrogen production by the electrolysis of plastic-waste was recently suggested as an alternative approach to water electrolysis, owing to its favoured thermodynamics. However, the fundamental aspects of such electro-catalytic process were not studied in detail. Here we propose a new approach to understand the electrolysis of polymers, by the use of model molecules. Our target is to develop a technology for the electrolysis of poly(methyl methacrylate), PMMA, plastic waste. We used methyl pivalate (MP) as a model molecule, since it contains similar functional groups than PMMA. We performed electrolysis experiments in a Polymer Electrolyte Membrane reactor with Nafion® protonic membranes and Pt/C electrodes at low temperatures (< 90ºC). The results obtained demonstrated that the electro-oxidation of MP allows to produce H_2 in a range of electrical potentials where water electrolysis is not thermodynamically possible (< 1.2 V). The kinetics of this process were studied and a preliminary global mechanism was proposed to explain the electro-oxidative cleavage of this model molecule. We have clearly demonstrated that the electrolysis of a plastic-like model monomer leads to the production of hydrogen. These results could be further extrapolated in view of the practical implementation of this technology for the valorisation of PMMA waste.

1. Introduction

The incursion of renewable energy sources in the electrical grid is an on-going process that will accelerate in the coming years. Renewable energy production (e.g. wind, hydraulic and solar) is increasing, but still fluctuating, making it challenging for their integration into the energy system [1]. To store these oscillating sources of energy and facilitate their transport, an energy carrier is required, hydrogen being the most promising one [2]. In this context, water electrolysis is one of the most popular electrochemical technologies that would allow transforming the renewable energies into pure H_2, with O_2 as the only by-product [3]. However, this process is not sustainable from energetic and economic points of view, since a minimum thermodynamic cell potential of 1.23 V is necessary to electrochemically cleave the H_2O molecule [4,5]. Consequently, different researchers have proposed to electrolyse organic molecules (e.g. methanol [6–9] and ethanol [10–15]), instead of water, to reduce the energy demand, since the thermodynamic potential for the electro-oxidation of these organic compounds is significantly lower than that for water. This opens the possibility for the use of organic wastes as a H_2 resource. Different organic wastes/by-products have already been studied in electrolysers such as wastewaters [16], biomass-based wastes [17–19], pyrolysis oil derivates [20], lignin [21–29] and glycerol [30,31].

In this frame, plastic-wastes are organic polymers and must also be contemplated as a massive source of hydrogen. Nowadays, less than 10 % and ~ 30 % of the plastics are recycled in USA and Europe, respectively [32,33]. In 2017, a considerable fraction of the plastic waste produced within the EU went to *Energy Recovery* (~ 39.5 %) [34] usually by direct combustion/incineration. However, this process often causes a significant environmental impact owing to hazardous emissions (NO_x, SO_x, Volatile Organic Compounds, etc.). The same year, the remaining vast amount of plastic waste was directly sent to landfill (~ 30.8 %) [34], which is not a viable option

in the long run. In addition, plastic wastes are becoming a major environmental issue in aquatic systems as a result of a permissible waste management and plastic fragmentation processes in the environment [35–38].

Among the different plastics, poly(methyl methacrylate) (PMMA) is a widely used polymer in automotive, construction and electrical industries, and is also crucial for the production of Plexiglass® and Perspex® [39]. The global market for this plastic is estimated to reach a value of about USD 11 billion for 2022 [40]. Even if different thermal and chemical methods are used today for recycling PMMA with a worthy recuperation rate of its monomer methyl methacrylate (MMA), no processes for direct *Energy Recovery* different than incineration are known. In the present study we propose, for the very first time, a novel potential route to valorise PMMA waste by producing H_2 via low temperature electrolysis.

The direct electrolysis of synthetic polymers for H_2 production has been scarcely studied. To the best of our knowledge, only two studies [41,42] reported the electrolysis of plastics (polypropylene) in high temperature Solid Oxide Electrolysers (> 800ºC). One study reported a solar thermo-coupled electrochemical depolymerization of polypropylene at intermediate temperatures (350-400 ºC) [43], and one study was recently carried out in low temperature (< 200ºC) electrolysers [44]. Low temperature electrolysers are advantageous in terms of simplicity and energy-demand. In ref. [44], a wide variety of industrial common plastics (sponges, cable ties, stocking and rope) and pure polymers (polyvinyl alcohol (PVA) and polyurethane) were electrolyzed in acid media (85% H_3PO_4) on Pt-based electrodes. Even though this study demonstrated the proof-of-concept to electrolyze plastic-waste resources in low temperature electrolysers, the electrochemical processes involved and mechanistic routes are not described. A deep comprehension of the processes involved will allow assessing the feasibility of the electrochemical cleavage of plastic polymer and the optimization of procedures to produce H_2 from

plastic-waste. In addition, we believe that the strong acid media could transform the polymer into smaller molecules easy to electrolyse, and therefore the process would not be purely electro-catalytic.

In the present study, we report a different approach to understand the mechanism for the electro-oxidation of PMMA. Due to the complexity and the heterogeneity of real PMMA-based plastics, a *model molecule* representative of the main chemical bonds present in the polymer repeating unit was used: methyl trimethylacetate (methyl pivalate, MP). This molecule exhibits identical ester units, together with the C=O, C-C and C-H bonds than in PMMA, as opposed to the monomer methyl methacrylate (MMA), which exhibits a double C=C bond absent in the polymer (Fig. S1). The MP model molecule is slightly soluble in water, allowing performing electrochemical experiments in aqueous phase as opposed to PMMA, which is a water-insoluble solid. The idea of this work is to study, for the first time, the electro-oxidation of the MP model molecule. To do that, we performed electrolysis experiments in a Polymer Electrolyte Membrane-based (PEM) reactor with acidic-based membranes which serve as electrolyte (Nafion®). This configuration allows working in aqueous media in the absence of a liquid electrolyte (e.g. H_3PO_4), then preserving the MP molecules in the anodic compartment. This study represents a starting point towards understanding the electrochemical cleavage of the main bonds present in the PMMA plastic, and the results could be further extrapolated for real plastic-wastes.

2. Experimental

The experiments were performed in a commercial Polymer Electrolyte Membrane (PEM) electrolysis cell (Dioxide Materials®) using commercial electrodes and membranes (FuelCellStore®). Both electrodes (5.3 cm^2) were composed of a Pt/C catalyst impregnated on a carbon cloth with a carbon gas diffusion layer (0.2 mg cm^{-2} of 20 % wt. Pt supported on C_{Vulcan}). A Nafion™ 117 membrane was used as proton-conducting membrane (183 µm thickness). Before

use, the membrane was pretreated by immersion at 100 °C for 2 h in 3 different solutions: 150 mL of 3 % wt. H_2O_2, then 150 mL of 0.5 M H_2SO_4 and finally 150 mL of deionized water. The membrane electrode assembly (MEA, anode/membrane/cathode) was prepared by hot-pressing under 1 metric ton at 120°C for 3 min. Then, the MEA was introduced between two Teflon gaskets to ensure correct sealing of the cell and the PEM cell assembly was mounted. A temperature control system and reactants/products flasks for anodic and cathodic compartments were put in place as well. Figure 1 shows the scheme of the PEM experimental set-up.

Methyl trimethylacetate (methyl pivalate, MP, 99 % purity, boiling point 110ºC, < 15 g L^{-1} solubility in water), trimethylacetic acid (pivalic acid, PA, 99 % purity) and methanol (MeOH, ≥ 99.9 % purity) were purchased from Sigma-Aldrich. During the electrolysis experiments, an aqueous solution of the model molecule (30 mL, 10 g L^{-1} methyl pivalate, 1000 rpm stirring, 1.8 mL min^{-1}) and deionized water (30 mL, 1.8 mL min^{-1}) were fed to the anode and cathode compartments, respectively. For comparison purposes, every experiment was first performed under the same conditions by feeding deionized water to both, anode and cathode. All solutions were fed in recirculation mode starting 30 min before applying polarization (for stabilization purposes). A peristaltic pump assured constant liquid flow rates. For the polarization of the PEM cell, a potentiostat-galvanostat equipped with a 10 A booster (Origalys®) was used.

In addition, the hydrogen purity and production was verified online with a quadrupole mass spectrometer (Portable Quadrupole MS, Aspec). The QMS operates with high vacuum of around $1.3x10^{-6}$ mbar, evacuated by a 70 L/s turbo molecular drag pump combined with a backing pump. The relative molecular concentrations of different compounds such as H_2 ($m/z = 2$ amu), H_2O (18 amu), N_2 (28 amu), O_2 (32 amu), and CO_2 (44 amu) were online monitored. The gas out-stream in the cathodic vessel (see Fig. 1) was mixed with a constant flow of inert gas (He, 33 mL min^{-1}) and

further introduced into the QMS device. The H_2 trend was analysed and expressed in arbitrary units.

3. Results and discussion

The first tests were performed to demonstrate the possibility to electrolyse the organic model molecule (MP) in a range of electrical potentials where water electrolysis is thermodynamically impossible, i.e., $V_{cell} < 1.23$ V. Fig. 2a shows the 10^{th} cycle of cyclic voltammetry experiments (V_{cell} = 0 - 1100 mV, scanning rate of 10 mV s^{-1}) by feeding deionized water or the MP solution to the anode, always in the absence of any liquid electrolyte, at 80ºC. With regards to water electrolysis, a trend observed in previous studies for Pt-based materials [27] was obtained, with a weak forward onset oxidation potential at ~ 0.9 V attributed to a partial passivation of Pt (formation of oxygen layer), which would be reduced during the backward scan.

The introduction of the organic model molecule leads to a completely different trend. First of all, much higher electrical currents (i.e. higher electrolysis efficiency) were obtained during both, forward and backward scans. As previously shown in Fig. 1 (PEM scheme), since acid H^+ membranes were used, MP solutions fed to the anode are electro-oxidized ($MP + H_2O \rightarrow MP_{ox} + 2H^+ + 2e^-$), with the subsequent production of oxidized products and H^+. The protons migrate through the membrane, leading to the corresponding H_2 evolution cathodic reaction ($2H^+ + 2e^- \rightarrow H_2$). Therefore, the enhanced performance of the electrolyser in the presence of MP can be clearly attributed to the electro-oxidation of the organic model molecule. In addition, during the forward scan, with an onset potential of ~ 400 mV, a significant oxidation peak was observed at ~ 700 mV. After that, the current decreased, and a new oxidation trend seemed to start around the maximum potential applied (1100 mV). During the backward scan, after an electrical current decrease, a new oxidation peak was obtained at a very similar potential than the forward peak (~ 750 mV). As a

matter of fact, similar trends were obtained for the electro-oxidation of simple alcohols (e.g. methanol [45], ethanol [46,47]) in Pt-based electrodes. The results obtained could be explained according to two different mechanisms:

i) the forward peak is usually due to the electro-oxidation of the organic molecule to some reaction intermediate, while the backward oxidation peak could be attributed to the oxidation of such reaction intermediate still adsorbed on the catalyst surface, as suggested for methanol in ref. [48].

ii) the backward oxidation peak could be just attributed to the adsorption of new molecules of the organic feedstock [45].

In the case of the present study, the second option seems more likely, considering that the oxidation peak for both, forward and backward scans, takes place at very similar cell potentials. If this is the case, it is worth mentioning that the backward peak is much smaller than the forward peak, which indicates that the catalyst surface might change upon the application of higher potentials, or some of the reaction intermediates produced during the forward scan remained chemisorbed on the catalyst, leading to a partial poisoning of the anodic Pt active sites.

The purity and production of hydrogen at the cathode was verified by mass-spectrometry (MS) measurements of the gas species produced. Fig. 2c shows the whole voltammetry experiment previously described (10 cycles) for the MP model molecule in dynamic mode, i.e., current vs. time, together with the variation of the MS signal for H_2 (in arbitrary units). As expected, considering the pure H^+ conductivity of Nafion membranes, no other gas product was detected at the cathode. In addition, it can be clearly observed that the hydrogen measured followed exactly the same trend than that for the current obtained in the cyclic voltammetry experiment. It points out that this powerful technique allows to correlate *in-operando* the obtained current with the production of pure hydrogen in this electrolysis technology.

To get more insights into the electrochemical behaviour of the MP electrolysis, chrono-amperometry experiments were performed under the same reaction conditions (Fig. 2b). Different potentials were applied in a range from 0 to 1100 mV (forward and backward) for 10 min each with a step change of 100 mV. During the forward experiments, a very similar trend than that observed for the cyclic voltammetry was obtained, with maximum currents at 700-800 mV. The cathodic H_2 production was calculated according to the Faraday's law ($r_{H_2} = \frac{j_p}{nF}$, where j_p is the current density obtained under polarization, n is the number of transferred electrons, *2* in this case, and F is the Faraday's constant). At every applied potential higher than 600 mV, the current suffered a strong decay with time. In addition, during the backward experiments (from 1100 to 0 mV), a similar trend was observed, but the obtained currents were slightly lower in general.

The obtained results suggest an enhanced performance for the electro-oxidation of the MP organic model molecule in a range of potentials were water electrolysis is simply not possible, i.e., ~ 700-800 mV. The following conclusions could be deduced from these figures: i) the trend observed could be rationalized as in a previous study by Wang et al. with ethanol on Pt electrodes [46], where they suggested that at high potentials the electro-oxidation of the organic could be hindered by the passivation/oxidation of Pt to PtO, in good agreement with the trend observed when water was fed to the system (Fig. 2a). During the backward scan, the electro-oxidation competes with PtO reduction, first leading to a current decrease, followed by the formation of a second oxidation peak. ii) together with the likely oxidation of Pt, the system seems to suffer a significant deactivation even in short periods of time, suggesting that the anodic Pt catalyst could be partially poisoned by some reaction intermediates or products produced at the optimum potentials. To support this hypothesis, long-run chrono-amperometric experiments were also carried out with a fresh MEA at different fixed potentials (500, 750 and 1000 mV) for 45 min. As shown in Fig. S2, the currents

obtained at 750 and 1000 mV were lower than in the above described experiment, which could be attributed to degradation of the catalyst during the long-run experiment at 500 mV. Nevertheless, these experiments show that the performance of the system decreased with the time at all the studied potentials, with a higher registered current when the PEM cell works at 750 mV, in good agreement with the experiments shown in Fig. 2b. A similar deactivation phenomenon was observed in previous studies for ethanol electrolysis on Pt-based electrodes [49,50]. In those studies, the catalyst was further regenerated by a cyclic strategy, by applying steady polarizations between 0 and 1 V forward and backwards until the activity was recovered. We demonstrated that the application of such potentials led to the further electro-oxidation of the poisonous species. Therefore, a similar cyclic strategy will be proposed in future studies aiming for the regeneration of the Pt catalyst used in this study.

Aiming for a study of the overall kinetics for the electro-oxidation of the MP model molecule, the influence of the MP concentration in the starting solution was studied. Fig. 3a shows a series of cyclic voltammetry experiments (V_{cell} = 0 - 1100 mV, scanning rate of 10 mV s^{-1}) at a constant temperature of 80ºC for the different MP concentrations. The maximum MP concentration tested was 10 g L^{-1} due to the limited solubility of MP in water. Even if a similar trend was observed for all the experiments, the electrochemical performance towards MP electro-oxidation clearly increased with its concentration in the initial solution. After each voltammetry experiment, a chrono-amperometry test was performed at each concentration upon the application of 750 mV for 30 min (Fig. 3b), where a growing current (and therefore H_2 production) was also obtained as the MP concentration increased.

Since the PEM device works in recirculation mode, it can be considered as a batch system, where the overall rate law can be simplified as [51]:

$$r_{H_2} = kC_{H_2O}^{a} C_b^{n} = k_{obs} C_b^{n} \quad (1)$$

Where k is the rate constant, C_{H_2O} and C_b are the initial H_2O and MP concentrations, and a and n are the reaction orders with respect to H_2O and MP, respectively. Assuming an almost constant water concentration due to the water excess in the initial solution, k_{obs} comprises the rate constant, together with the concentration of water. According to Eq. 1, the representation $ln(r_{H_2})$ vs. $ln(C_b)$ leads to a linear fit, and its slope corresponds to the reaction order n. Fig. 3c depicts the average r_{H_2} (obtained by integrating the curves shown in Fig. 3b, divided by the duration of the experiment) vs. the initial MP concentration, while the inset in such figure displays the logarithm fit. The reaction order observed was $n \approx 1$. These results clearly demonstrate that the system is not governed by diffusional limitations, and that the production of hydrogen is strongly dependent on the concentration of the model molecule. In this sense, and considering the limited solubility of MP in water, an initial concentration of 10 g L^{-1} was chosen for the rest of the experiments of this study.

In the next series of experiments, the influence of the reaction temperature was studied for the electrolysis of the MP model molecule. Figures 4a and b show, respectively, cyclic voltammetry (V_{cell} = 0 - 1100 mV, scanning rate of 10 mV s^{-1}) and chrono-amperometry experiments (0 to 1100 mV, step change of 100 mV, 10 min at each potential) at 50, 70 and 80 ºC. Experiments at higher temperatures were not performed in order to avoid the partial evaporation of the anodic solution. Similar trends were observed in both figures for all the reaction temperatures. However, the activity of the system seems to be almost negligible at 50 ºC. As expected, higher temperatures improved the overall performance. It can be attributed to two factors: the enhanced ionic conductivity of the polymer electrolyte membrane and the acceleration of electro-oxidation kinetics. A similar phenomenon was observed in a previous study for lignin electrolysis [27] (a complex organic bio-polymer), where a temperature of at least 50ºC was required to activate the electro-oxidation of the

organic molecule. However, the electrolysis of simple organic alcohols (e.g. methanol, ethanol and glycerol) is known to take place even at room temperature. It seems to indicate that the electro-oxidation of complex organic molecules, such as MP, needs to overcome significant kinetic barriers. In this context, the activation energies for the oxidation processes were calculated by the Arrhenius equation (Fig. 4c):

$$k = Ae^{\left[-\frac{E_a}{RT}\right]} \quad (2)$$

Where k is the rate constant, A is a pre-exponential factor, E_a is the activation energy, T is the temperature and R is the gas constant. The Arrhenius plots ($ln\ r_{H2}$ vs. $1/T$) were obtained by using the hydrogen production (calculated from the current values by the Faraday's law) at the maximum values of the forward and backward electro-oxidation peaks previously discussed (Fig. 4a). E_a values of 42.6 kJ mol^{-1} (forward scan, V_{cell} ~ 700 mV) and 55.9 kJ mol^{-1} (backward scan, V_{cell} ~ 700 mV) were calculated, respectively. Several factors affect the activation energy calculation, including the applied potential. For instance, values between 10 and 25 kJ mol^{-1} [52,53] have been reported for methanol electro-oxidation on Pt/C electrodes at 0.5-0.7 V. These results suggest that the electro-oxidation observed during the backward scan needs to overcome a more energetic barrier than the forward electro-oxidation. It could be due to the fact that the electro-oxidation of MP takes places in several consecutive steps, and therefore those peaks could be attributed to different reactions. Nevertheless, as previously explained, it could also be attributed to the partial passivation/oxidation of Pt at high potentials during the forward scan, which would hinder the MP electro-oxidation during the backward scan. In any case, it seems that the electro-oxidation of the model organic molecule is limited at low reaction temperatures, and higher activation energies than those previously reported for methanol on similar anode materials are required.

During the electro-oxidation of alcohols more complex than methanol on Pt-based materials, such as ethanol, the cleavage of the molecule generally leads to its partial oxidation towards aldehyde and carboxylic acids at similar temperatures and upon the application of low electrical potentials (< 1.23 V). That indicates that the activity of the system is limited to the oxidation of the alcohol (-OH) terminal functional groups. However, the MP molecule does not have –OH terminal bonds in its structure (nor the PMMA polymer, see Fig. S1). Therefore, considering that C-C cleavage seems very unlikely under such conditions [46,54,55], we propose that the electro-oxidation activity observed in Figs. 2-5 is linked to the electro-oxidative cleavage of the ester C-O bonds, as we will explain later in the manuscript. All in all, these experiments prove that, potentially, the electrolysis of the PMMA plastic polymer is possible in a range of potentials lower than that for pure water electrolysis. Further analysis of the charge transfer kinetics for MP electro-oxidation was performed by varying the scanning rates during cyclic voltammetry experiments. Fig. 5a shows the voltammograms (10^{th} cycle) at scanning rates between 10 and 50 mV/s, by feeding solutions of MP to the anode (10 g L^{-1}) at 80 ºC. The full voltammetry experiments are shown in Fig. S3.

As expected, faster scan rates lead to higher electrical currents during the forward scan (and slightly lower currents during the backward scan) due to a decrease of the diffusion layer size. As previously reported for the electrolysis of other organic molecules (e.g. ethanol [56] and lignin [57]), the electro-oxidation of MP is most likely an irreversible process. As discussed by Han et al. [56], the peak potential exhibits a linear dependence upon the logarithm of the square root of the scanning rate if the reaction is irreversible, as is the case in this study (see inset in Fig. 5a). Therefore, following a similar approach than Movil et al. [57] for totally irreversible one-step/one-electron reactions (described in detail in ref. [58]), we calculated the standard charge transfer rate constant (k^0) for the two main electro-oxidation processes observed during the forward (k^0_1) and the backward (k^0_2) scans by using equation 3:

$$I_p = nAFk^0 C_b e^{\left[-\frac{\alpha F}{RT}(E_p - E^{0'})\right]} \quad (3)$$

Where I_p is the current obtained at the peak, A is the area of the electrode, α is the transfer coefficient, C_b is the reactant concentration, E_p is the peak potential and $E^{0'}$ is the formal potential (standard electrode potential under specific reaction conditions). Considering a low degree of consumption of MP compared to its high initial concentration (10 g L^{-1}), C_b was assumed to be constant. In addition, since no values of $E^{0'}$ could be found in literature for the MP model molecule, we will keep the same assumption of Movil et al. [57], considering the formal electrode potential for MP is the same than that for carbon (0.21 V vs. SHE). Taking the I_p and E_p data for both oxidation peaks at different scanning rates, a linearization of Eq. 3 can be done in the form of $ln(i_p)$ vs. $(E_p\text{-}E^{0'})$. The plots are shown in Fig. 5b, where the intercept of each line is equal to $ln(nAFk^0C_b)$. It allows calculating the following k^0 values: k^0_1=4.74x10^{-3} cm s^{-1} and k^0_2=1.58x10^{-6} cm s^{-1} for the forward and backward peaks, respectively. The physical interpretation of these values is associated with the kinetic facility of the redox couple. In other words, high k^0 values indicate that the system will rapidly achieve the equilibrium. Both values of k^0 fall in the intermediate range, considering common k_0 values between 1-10 (for fast processes) and 10^{-9} (for slow processes) [58]. The standard charge transfer rate constant range of our investigated electrochemical system is typical of irreversible reactions. Hence, the results obtained suggest that the forward peak is related to an electro-oxidation process with simpler and faster transfer of electrons than the backward peak. Two assumptions can be proposed: i) the competition between the reduction of oxidized Pt and the MP electro-oxidation reaction during the backward scan, or ii) the formation of strongly adsorbed species during the forward scan, which would hinder the kinetics of the electro-oxidation process during the backward scan.

Having in mind the irreversible nature of the MP electro-oxidation process, a preliminary global reaction mechanism can be proposed. From previous studies on electrolysis of other small organic molecules (e.g. ethanol [46,54,55] and glycerol [59,60]), we can assume that cleaving C-C bonds is very unlikely at low temperatures and applied potentials < 1.2 V. In addition, it is well-known that acid hydrolysis of esters is simply the reverse of the esterification process, leading to the formation of a carboxylic acid and an alcohol [61] (*R-C=O-O-R' + H_2O → R-C=O-OH + R'-OH*). As the MP electrolysis is carried out in a PEM cell with an acid membrane in the absence of any liquid electrolyte, the cleavage of the MP model molecule is purely (or mainly) electrochemical, as opposed to the reference study recently published for plastic electrolysis [44], where the plastic could be potentially transformed into smaller molecules in the H_3PO_4 liquid electrolyte. Hence, we believe that the electro-oxidation of MP is most likely due to the cleavage of the ester group, leading to the production of a carboxylic acid (pivalic acid, PA) and intermediate methoxy-type species (CH_3O-), in a similar way than the esters acid hydrolysis previously described. The methoxy intermediate species would be further oxidized into CO_2, with the subsequent production of H^+ and e^-, which would further migrate to the cathode to produce hydrogen, as represented by the following equations:

$$Anode: (CH_3)_3CCOOCH_3 + 2\,H_2O \rightarrow (CH_3)_3CCOOH + CO_2 + 6H^+ + 6e^- \quad (4)$$

$$Cathode: 6H^+ + 6e^- \rightarrow 3H_2 \quad (5)$$

In order to support this overall reaction mechanism, cyclic voltammetry experiences (10th cycle) with aqueous solutions of methanol and pivalic acid (in the absence of liquid electrolyte) were performed at 80ºC, using the stoichiometric concentrations corresponding to a total conversion of a MP 10 g L^{-1} solution, i.e. 0.086 mol L^{-1} (Fig. 6). Regarding the methanol curve, it is worth noting its similar trend compared to the MP electro-oxidation, with forward and backward peaks appearing at similar potentials, even though the obtained current was higher for methanol. This could be

attributed to the higher activation energy (i.e., the higher kinetic barrier) observed for the electrolysis of the MP model molecule, compared to that previously reported for direct methanol electrolysis. On the other hand, no activity was obtained for the electrolysis of pivalic acid under the proposed working conditions. This is expected, considering that the further oxidation of carboxylic acid at low potentials and reaction temperatures is very unlikely, as previously observed for the electrolysis of ethanol on Pt-based catalyst-electrodes. Therefore, these experiments agree with the global mechanism proposed by Eqs. 4 and 5. Considering this initial theory, MP seems to be the right model molecule as a representative of PMMA. Taking into account the unlikely C-C cleavage, the electrochemical depolymerization of PMMA can be disregarded under the studied reaction conditions with the Pt/C catalyst. The above-suggested electrochemical cleavage of the ester functional group, leading to the production of methoxy groups (which would be further electro-oxidized leading to the production of H_2), could potentially happen in an important extent with the PMMA with similar energy requirements, without breaking the polymer backbone chain. Despite, other issues should be taking into consideration, including the fact that PMMA is not soluble in water and therefore such material should be pretreated or introduced in form of nano-dispersions to minimize the very likely diffusional limitations. In any case, further experiments will be performed in future studies coupled with products analysis by liquid chromatography and spectroscopic techniques to corroborate the fundamental aspects of this original system.

4. Conclusions

This study reports the electrochemical behaviour for the electro-oxidation of MP, an organic model molecule with similar bonds than the PMMA polymer, on Pt-based electrodes. First of all, we clearly demonstrated that the electro-oxidation of this molecule leads to an enhanced performance compared to water electrolysis at low temperatures (50-80ºC) and in a low range of electrical potentials (< 1.2 V). The highest electrochemical performances for MP electro-oxidation were

achieved at intermediate reaction potentials (700-800 mV), where the partial oxidation of Pt did not occur. However the system suffered a significant deactivation with time, likely owing to the strong chemisorption of reaction intermediates or products. All in all, this study establishes a starting point towards understanding the electro-catalytic transformation of MP, allowing for the production of H_2 (most likely) from the cleavage of the ester groups. These results could be extrapolated to PMMA, in view of the further valorisation of the massive amounts of this kind of plastic waste to produce pure green hydrogen.

5. Acknowledgments

The authors gratefully acknowledge the French institution “Ecole Urbaine de Lyon” (EUL - Institut de Convergences) for funding a PhD grant offered to the leading author of this study, Mr. Grimaldos-Osorio.

References

[1] Bareiß K, de la Rua C, Möckl M, Hamacher T. Life cycle assessment of hydrogen from proton exchange membrane water electrolysis in future energy systems. Appl Energy 2019;237:862–72. https://doi.org/10.1016/j.apenergy.2019.01.001.

[2] Züttel A, Remhof A, Borgschulte A, Friedrichs O. Hydrogen: The future energy carrier. Philos Trans R Soc A Math Phys Eng Sci 2010;368:3329–42. https://doi.org/10.1098/rsta.2010.0113.

[3] Shiva Kumar S, Himabindu V. Hydrogen production by PEM water electrolysis – A review. Mater Sci Energy Technol 2019;2:442–54. https://doi.org/10.1016/j.mset.2019.03.002.

[4] Buttler A, Spliethoff H. Current status of water electrolysis for energy storage, grid balancing and sector coupling via power-to-gas and power-to-liquids: A review. Renew Sustain Energy Rev 2018;82:2440–54. https://doi.org/10.1016/j.rser.2017.09.003.

[5] Coutanceau C, Baranton S. Electrochemical conversion of alcohols for hydrogen production: a short overview. Wiley Interdiscip Rev Energy Environ 2016;5:388–400. https://doi.org/10.1002/wene.193.

[6] Guenot B, Cretin M, Lamy C. Clean hydrogen generation from the electrocatalytic oxidation of methanol inside a proton exchange membrane electrolysis cell (PEMEC): effect of methanol concentration and working temperature. J Appl Electrochem 2015;45:973–81. https://doi.org/10.1007/s10800-015-0867-3.

[7] Lamy C, Guenot B, Cretin M, Pourcelly G. A Kinetics Analysis of Methanol Oxidation under Electrolysis/Fuel Cell Working Conditions. ECS Trans 2015;66:1–12. https://doi.org/10.1149/06629.0001ecst.

[8] Pham AT, Baba T, Sugiyama T, Shudo T. Efficient hydrogen production from aqueous

methanol in a PEM electrolyzer with porous metal flow field: Influence of PTFE treatment of the anode gas diffusion layer. Int J Hydrogen Energy 2013;38:73–81. https://doi.org/10.1016/j.ijhydene.2012.10.036.

[9] Uhm S, Jeon H, Kim TJ, Lee J. Clean hydrogen production from methanol-water solutions via power-saved electrolytic reforming process. J Power Sources 2012;198:218–22. https://doi.org/10.1016/j.jpowsour.2011.09.083.

[10] Caravaca A, Sapountzi FM, De Lucas-Consuegra A, Molina-Mora C, Dorado F, Valverde JL. Electrochemical reforming of ethanol-water solutions for pure H <inf>2</inf> production in a PEM electrolysis cell. Int J Hydrogen Energy 2012;37. https://doi.org/10.1016/j.ijhydene.2012.03.062.

[11] Gutiérrez-Guerra N, Jiménez-Vázquez M, Serrano-Ruiz JC, Valverde JL, de Lucas-Consuegra A. Electrochemical reforming vs. catalytic reforming of ethanol: A process energy analysis for hydrogen production. Chem Eng Process Process Intensif 2015;95:9–16. https://doi.org/10.1016/j.cep.2015.05.008.

[12] Gutiérrez-Martín F, Calcerrada AB, de Lucas-Consuegra A, Dorado F. Hydrogen storage for off-grid power supply based on solar PV and electrochemical reforming of ethanol-water solutions. Renew Energy 2020;147:639–49. https://doi.org/10.1016/j.renene.2019.09.034.

[13] Ruiz-López E, Amores E, Raquel de la Osa A, Dorado F, de Lucas-Consuegra A. Electrochemical reforming of ethanol in a membrane-less reactor configuration. Chem Eng J 2020;379:122289. https://doi.org/10.1016/j.cej.2019.122289.

[14] Lamy C, Jaubert T, Baranton S, Coutanceau C. Clean hydrogen generation through the electrocatalytic oxidation of ethanol in a Proton Exchange Membrane Electrolysis Cell (PEMEC): Effect of the nature and structure of the catalytic anode. J Power Sources

2014;245:927–36. https://doi.org/10.1016/j.jpowsour.2013.07.028.

[15] Caravaca A, De Lucas-Consuegra A, Calcerrada AB, Lobato J, Valverde JL, Dorado F. From biomass to pure hydrogen: Electrochemical reforming of bio-ethanol in a PEM electrolyser. Appl Catal B Environ 2013;134–135:302–9. https://doi.org/10.1016/j.apcatb.2013.01.033.

[16] Cheng W, Singh N, Maciá-Agulló JA, Stucky GD, McFarland EW, Baltrusaitis J. Optimal experimental conditions for hydrogen production using low voltage electrooxidation of organic wastewater feedstock. Int J Hydrogen Energy 2012;37:13304–13. https://doi.org/10.1016/j.ijhydene.2012.06.073.

[17] Chen YX, Lavacchi A, Miller HA, Bevilacqua M, Filippi J, Innocenti M, et al. Nanotechnology makes biomass electrolysis more energy efficient than water electrolysis. Nat Commun 2014;5. https://doi.org/10.1038/ncomms5036.

[18] Hibino T, Kobayashi K, Ito M, Ma Q, Nagao M, Fukui M, et al. Efficient Hydrogen Production by Direct Electrolysis of Waste Biomass at Intermediate Temperatures. ACS Sustain Chem Eng 2018;6:9360–8. https://doi.org/10.1021/acssuschemeng.8b01701.

[19] Crisafulli R, de Lino Amorim FM, de Oliveira Marcionilio SML, Mendes Cunha W, S. de Araújo BR, Dias JA, et al. Electrochemistry for biofuels waste valorization: Vinasse as a reducing agent for Pt/C and its application to the electrolysis of glycerin and vinasse. Electrochem Commun 2019;102:25–30. https://doi.org/10.1016/j.elecom.2019.03.012.

[20] Brueckner TM, Hawboldt KA, Pickup PG. Electrolysis of pyrolysis oil distillates and permeates in a multi-anode proton exchange membrane cell. Appl Catal B Environ 2019;256:117892. https://doi.org/10.1016/j.apcatb.2019.117892.

[21] Lalvani SB, Rajagopal P. Lignin-Augmented Water Electrolysis. J Electrochem Soc 1992;139:L1–2. https://doi.org/10.1149/1.2069212.

[22] Lalvani SB, Rajagopal R. Hydrogen production from lignin-water solution by electrolysis. Holzforschung 1993;47:283–6. https://doi.org/10.1515/hfsg.1993.47.4.283.

[23] Roy Ghatak H. Electrolysis of black liquor for hydrogen production: Some initial findings. Int J Hydrogen Energy 2006;31:934–8. https://doi.org/10.1016/j.ijhydene.2005.07.013.

[24] Ghatak HR, Kumar S, Kundu PP. Electrode processes in black liquor electrolysis and their significance for hydrogen production. Int J Hydrogen Energy 2008;33:2904–11. https://doi.org/10.1016/j.ijhydene.2008.03.051.

[25] Movil O, Garlock M, Staser JA. Non-precious metal nanoparticle electrocatalysts for electrochemical modification of lignin for low-energy and cost-effective production of hydrogen. Int J Hydrogen Energy 2015;40:4519–30. https://doi.org/10.1016/j.ijhydene.2015.02.023.

[26] Hibino T, Kobayashi K, Nagao M, Teranishi S. Hydrogen Production by Direct Lignin Electrolysis at Intermediate Temperatures. ChemElectroChem 2017;4:3032–6. https://doi.org/10.1002/celc.201700917.

[27] Caravaca A, Garcia-Lorefice WE, Gil S, de Lucas-Consuegra A, Vernoux P. Towards a sustainable technology for H<inf>2</inf> production: Direct lignin electrolysis in a continuous-flow Polymer Electrolyte Membrane reactor. Electrochem Commun 2019;100. https://doi.org/10.1016/j.elecom.2019.01.016.

[28] Bateni F, NaderiNasrabadi M, Ghahremani R, Staser JA. Low-cost nanostructured electrocatalysts for hydrogen evolution in an anion exchange membrane lignin electrolysis cell. J Electrochem Soc 2019;166:F1037–46. https://doi.org/10.1149/2.0221914jes.

[29] NaderiNasrabadi M, Bateni F, Chen Z, Harrington PB, Staser JA. Biomass-depolarized electrolysis. J Electrochem Soc 2019;166:E317–22. https://doi.org/10.1149/2.1471910jes.

[30] Simões M, Baranton S, Coutanceau C. Electrochemical valorisation of glycerol.

ChemSusChem 2012;5:2106–24. https://doi.org/10.1002/cssc.201200335.

[31] Kongjao S, Damronglerd S, Hunsom M. Electrochemical reforming of an acidic aqueous glycerol solution on Pt electrodes. J Appl Electrochem 2011;41:215–22. https://doi.org/10.1007/s10800-010-0226-3.

[32] Kunwar B, Cheng HN, Chandrashekaran SR, Sharma BK. Plastics to fuel: a review. Renew Sustain Energy Rev 2016;54:421–8. https://doi.org/10.1016/j.rser.2015.10.015.

[33] Rahimi A, García JM. Chemical recycling of waste plastics for new materials production. Nat Rev Chem 2017;1:1–11. https://doi.org/10.1038/s41570-017-0046.

[34] Lopez G, Artetxe M, Amutio M, Bilbao J, Olazar M. Thermochemical routes for the valorization of waste polyolefinic plastics to produce fuels and chemicals. A review. Renew Sustain Energy Rev 2017;73:346–68. https://doi.org/https://doi.org/10.1016/j.rser.2017.01.142.

[35] Al-Salem SM, Lettieri P, Baeyens J. Recycling and recovery routes of plastic solid waste (PSW): A review. Waste Manag 2009;29:2625–43. https://doi.org/10.1016/j.wasman.2009.06.004.

[36] Singh N, Hui D, Singh R, Ahuja IPS, Feo L, Fraternali F. Recycling of plastic solid waste: A state of art review and future applications. Compos Part B Eng 2017;115:409–22. https://doi.org/10.1016/j.compositesb.2016.09.013.

[37] Schwarz AE, Ligthart TN, Boukris E, van Harmelen T. Sources, transport, and accumulation of different types of plastic litter in aquatic environments: A review study. Mar Pollut Bull 2019;143:92–100. https://doi.org/10.1016/j.marpolbul.2019.04.029.

[38] Moura MRF, Falcão SMP, da Silva AC, Neto AR, Montenegro SMGL, da Silva SR. Developing a plastic waste management program: From river basins to urban beaches (case study). J Eng Technol Sci 2020;52:108–20.

https://doi.org/10.5614/j.eng.technol.sci.2020.52.1.8.

[39] Achilias DS. Chemical Recycling of Polymers. The Case of Poly(methyl methacrylate). Int Conf Energy Environ Syst 2006;2006:271–6.

[40] Godiya CB, Gabrielli S, Materazzi S, Pianesi MS, Stefanini N, Marcantoni E. Depolymerization of waste poly(methyl methacrylate) scraps and purification of depolymerized products. J Environ Manage 2019;231:1012–20. https://doi.org/10.1016/j.jenvman.2018.10.116.

[41] Pati S, Gopalan S, Pal UB. A solid oxide membrane electrolyzer for production of hydrogen and syn-gas from steam and hydrocarbon waste in a single step. Int J Hydrogen Energy 2011;36:152–9. https://doi.org/https://doi.org/10.1016/j.ijhydene.2010.10.013.

[42] Pal UB, Pati S, Yoong KJ, Gopalan S. (Invited) Electrolyzer for Waste to Energy Conversion. ECS Trans 2012;41:93–101.

[43] Jiang T, Zhao X, Gu D, Yan C, Jiang H, Wu H, et al. STEP polymer degradation: Solar thermo-coupled electrochemical depolymerization of plastics to generate useful fuel plus abundant hydrogen. Sol Energy Mater Sol Cells 2020;204. https://doi.org/10.1016/j.solmat.2019.110208.

[44] Hori T, Kobayashi K, Teranishi S, Nagao M, Hibino T. Fuel cell and electrolyzer using plastic waste directly as fuel. Waste Manag 2020;102:30–9. https://doi.org/10.1016/j.wasman.2019.10.019.

[45] Chung DY, Lee K-J, Sung Y-E. Methanol electro-oxidation on the Pt surface: Revisiting the cyclic voltammetry interpretation. J Phys Chem C 2016;120:9028–35. https://doi.org/10.1021/acs.jpcc.5b12303.

[46] Wang H, Jusys Z, Behm RJ. Ethanol electrooxidation on a carbon-supported Pt catalyst: Reaction kinetics and product yields. J Phys Chem B 2004;108:19413–24.

https://doi.org/10.1021/jp046561k.

[47] Pushkarev AS, Pushkareva IV, Ivanova NA, Du Preez SP, Bessarabov D, Chumakov RG, et al. Pt/c and pt/snox/c catalysts for ethanol electrooxidation: Rotating disk electrode study. Catalysts 2019;9. https://doi.org/10.3390/catal9030271.

[48] Manoharan R, Goodenough JB. Methanol oxidation in acid on ordered NiTi. J Mater Chem 1992;2:875–87.

[49] Caravaca A, De Lucas-Consuegra A, Calcerrada AB, Lobato J, Valverde JL, Dorado F. From biomass to pure hydrogen: Electrochemical reforming of bio-ethanol in a PEM electrolyser. Appl Catal B Environ 2013;134–135. https://doi.org/10.1016/j.apcatb.2013.01.033.

[50] Caravaca A, Sapountzi FM, De Lucas-Consuegra A, Molina-Mora C, Dorado F, Valverde JL. Electrochemical reforming of ethanol-water solutions for pure H<inf>2</inf>production in a PEM electrolysis cell. Int J Hydrogen Energy 2012;37:9504–13. https://doi.org/10.1016/j.ijhydene.2012.03.062.

[51] Caravaca A, Jones W, Hardacre C, Bowker M. H2 production by the photocatalytic reforming of cellulose and raw biomass using Ni, Pd, Pt and Au on titania. Proc R Soc A Math Phys Eng Sci 2016;472. https://doi.org/10.1098/rspa.2016.0054.

[52] Jing M, Jiang L, Yi B, Sun G. Comparative study of methanol adsorption and electro-oxidation on carbon-supported platinum in acidic and alkaline electrolytes. J Electroanal Chem 2013;688:172–9. https://doi.org/10.1016/J.JELECHEM.2012.10.028.

[53] Wakabayashi N, Uchida H, Watanabe M. Temperature-dependence of methanol oxidation rates at PtRu and Pt electrodes. Electrochem Solid-State Lett 2002;5. https://doi.org/10.1149/1.1513021.

[54] A. Monyoncho E, N. Steinmann S, Michel C, A. Baranova E, K. Woo T, Sautet P. Ethanol

Electro-oxidation on Palladium Revisited Using Polarization Modulation Infrared Reflection Absorption Spectroscopy (PM-IRRAS) and Density Functional Theory (DFT): Why Is It Difficult To Break the C–C Bond? ACS Catal 2016;6:4894–906. https://doi.org/10.1021/acscatal.6b00289.

[55] Monyoncho EA, Steinmann SN, Sautet P, Baranova EA, Michel C. Computational screening for selective catalysts: Cleaving the CC bond during ethanol electro-oxidation reaction. Electrochim Acta 2018;274:274–8. https://doi.org/10.1016/J.ELECTACTA.2018.04.102.

[56] Han L, Ju H, Xu Y. Ethanol electro-oxidation: Cyclic voltammetry, electrochemical impedance spectroscopy and galvanostatic oscillation. Int J Hydrogen Energy 2012;37:15156–63. https://doi.org/10.1016/J.IJHYDENE.2012.08.034.

[57] Movil O, Garlock M, Staser JA. Non-precious metal nanoparticle electrocatalysts for electrochemical modification of lignin for low-energy and cost-effective production of hydrogen. Int J Hydrogen Energy 2015;40:4519–30. https://doi.org/10.1016/j.ijhydene.2015.02.023.

[58] Bard A, Faulkner L. Electrochemical Methods: Fundamentals and Applications, 2nd Edition. Wiley Glob. New York: 2000.

[59] Coutanceau C, Baranton S, Kouamé RSB. Selective electrooxidation of glycerol into value-added chemicals: A short overview. Front Chem 2019;7. https://doi.org/10.3389/fchem.2019.00100.

[60] Simões M, Baranton S, Coutanceau C. Electrochemical valorisation of glycerol. ChemSusChem 2012;5:2106–24. https://doi.org/10.1002/cssc.201200335.

[61] Anantakrishnan SV, Krishnamurti S. Kinetic studies in ester hydrolysis - Part I. The hydrolysis of halogeno-aliphatic esters. Proc Indian Acad Sci - Sect A 1941;14:270–8.

https://doi.org/10.1007/BF03046068.

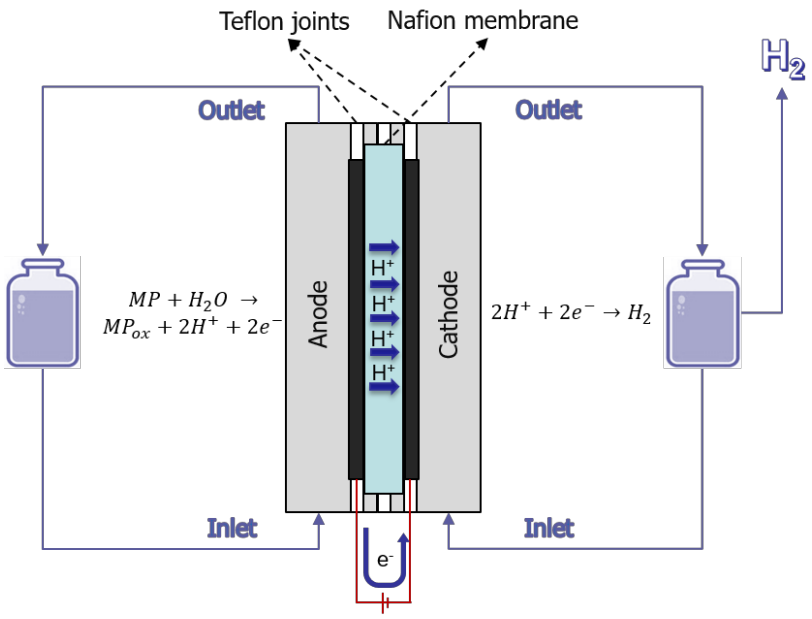

Figure 1. General scheme of the Polymer Electrolyte Membrane-based (PEM) experimental set-up used in this study, together with the global electrode reactions.

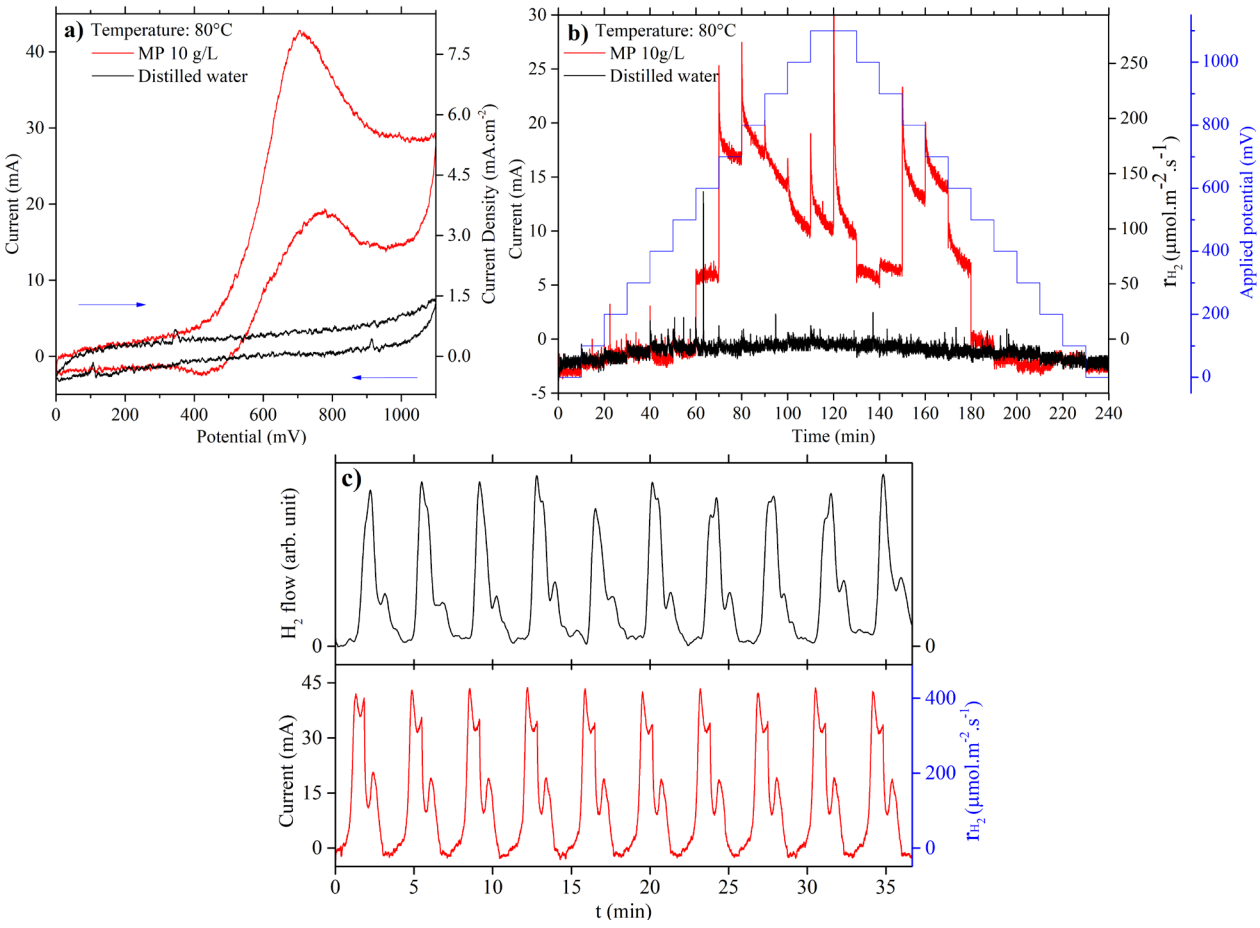

Figure 2. Comparison between MP and water electrolysis in a PEM cell: a) Cyclic voltammetry (scan rate 10 mV s^{-1}) from 0 to 1100 mV (only 10^{th} cycle), b) Chrono-amperometry from 0 to 1100 mV (forward and backward) under a step change of 100 mV (10 min at each potential), c) In-situ H_2 measuring by mass spectrometry (He dilution flow of 33 mL min^{-1}) during a cyclic voltammetry (scan rate 10 mV s^{-1}) from 0 to 1100 mV. Anode: MP 10 g L^{-1} in distillate water (MP electrolysis) or distillate water (water electrolysis), 30 mL solution, 1.8 mL min^{-1}. Cathode: distillate water, 30 mL, 1.8 mL min^{-1}. Temperature = 80ºC.

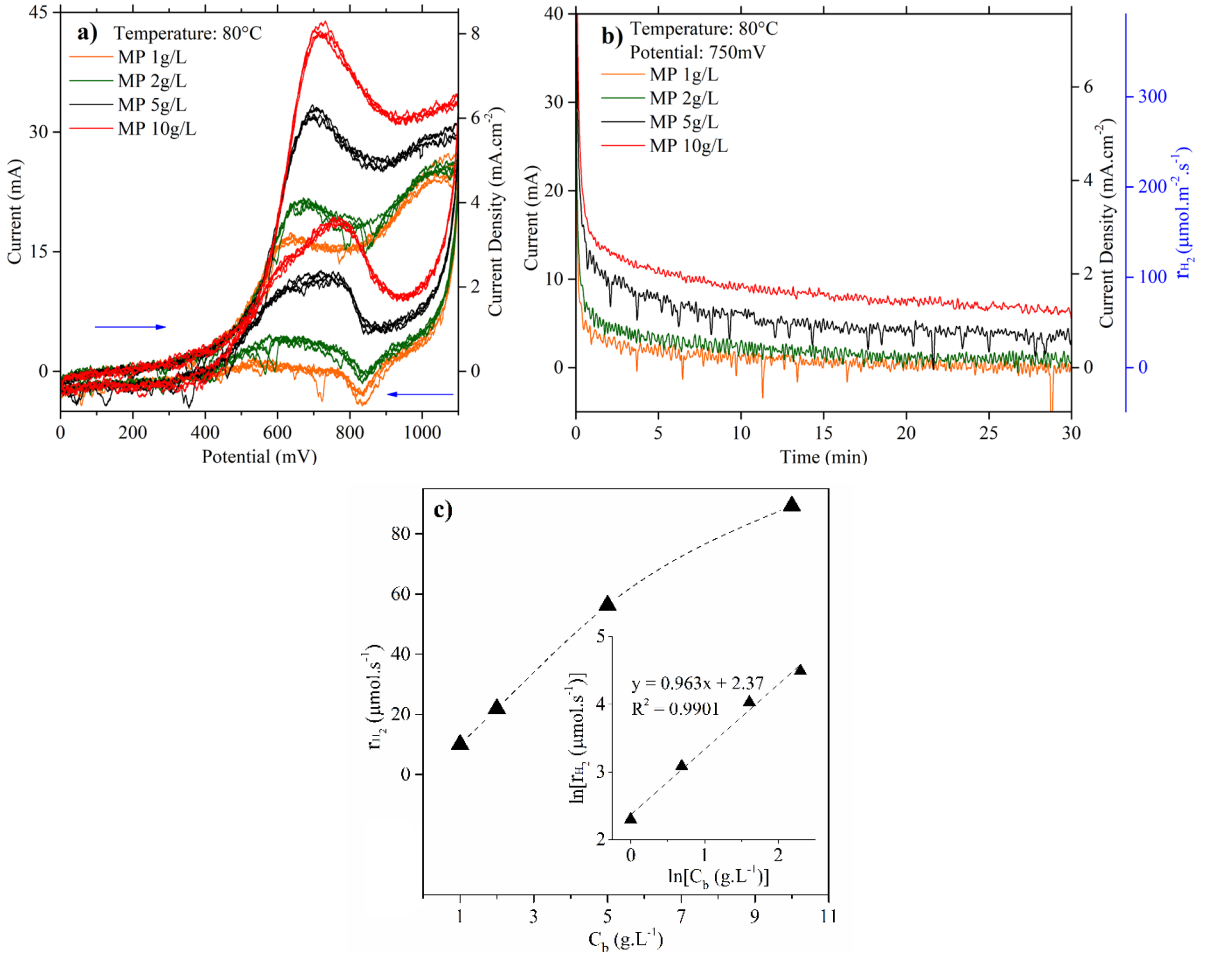

Figure 3. Effect of the concentration (C_b) on the MP electrolysis in a PEM cell: a) Cyclic voltammetry (scan rate 10 mV s^{-1}) from 0 to 1100 mV (only 4^{th}, 6^{th}, 8^{th} and 10^{th} cycles), b) Chrono-amperometry at 750 mV during 30 min, c) Influence of the initial MP concentration on the H_2 production and reaction order calculated from CA experiences (inset). Anode: MP 10 g L^{-1} in distillate water, 30 mL solution, 1.8 mL min^{-1}. Cathode: distillate water, 30 mL, 1.8 mL min^{-1}. Temperature = 80ºC.

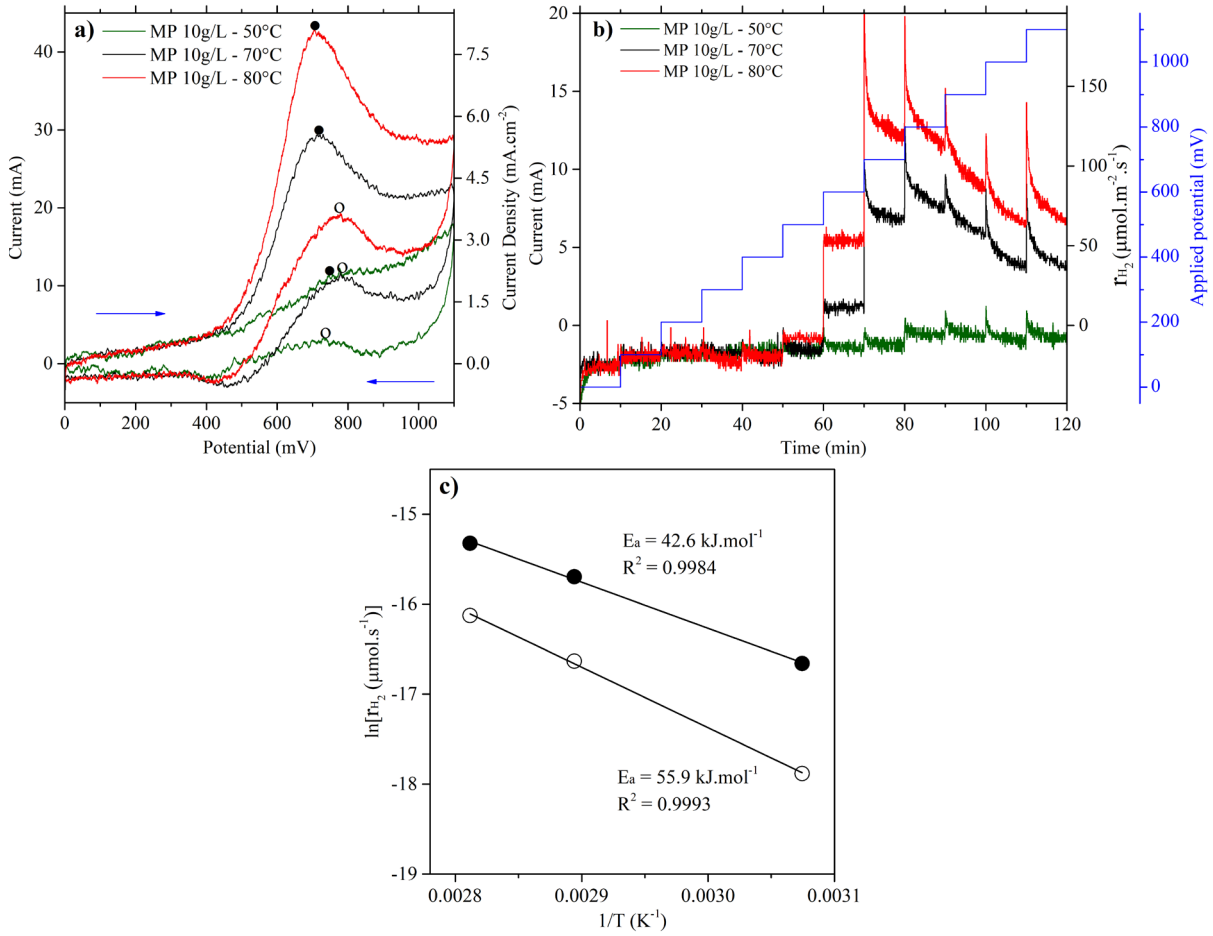

Figure 4. Effect of the reaction temperature on MP electrolysis in a PEM cell: a) Cyclic voltammetry (scan rate 10 mV s^{-1}) from 0 to 1100 mV (only 10th cycle), b) Chrono-amperometry from 0 to 1100 mV under a step change of 100 mV (10 min at each potential). c) Arrhenius plots: *ln* r_{H2} *vs. 1/T* (● forward peaks, ○ backward peaks). The calculations were made by using the data from Fig. 4a and the slope of the fit corresponds to -Ea/R (where R = 8.314 J.mol^{-1}.K^{-1}). Anode: MP 10 g L^{-1} in distillate water, 30 mL solution, 1.8 mL min^{-1}. Cathode: distillate water, 30 mL, 1.8 mL min^{-1}. Temperature = 50-80ºC.

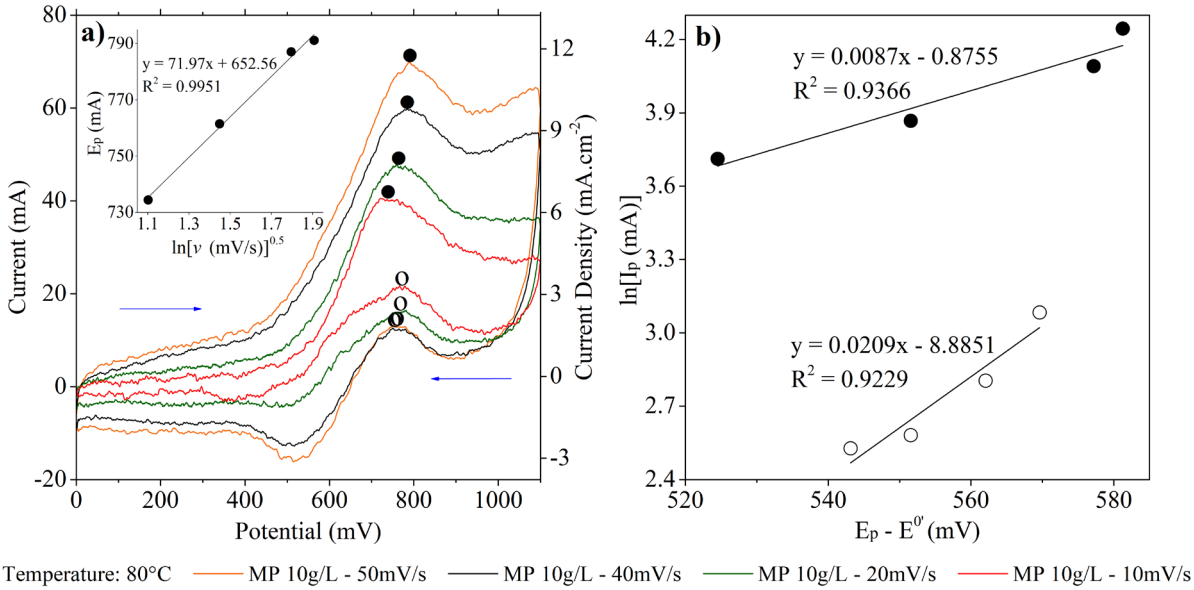

Figure 5. Effect of the scanning rate on MP electrolysis in a PEM cell: a) Cyclic voltammetry (scan rate 10-50 mV s^{-1}) from 0 to 1100 mV (only the 10th cycle). Inset figure: E_p *vs. Ln* ($\nu^{1/2}$) plot, where E_p is the potential of the forward peaks, and ν is the scan rate: a linear trend indicates the irreversibility of the electro-oxidation process. b) $ln(I_p)$ *vs.* $(E_p\text{-}E^{0'})$ plot, where I_p and E_p are the current and potential at the forward (•) and backward peaks (○) (Fig. 5a). The intercept allows for k^0 calculations. Anode: MP 10 g L^{-1} in distillate water, 30 mL solution, 1.8 mL min^{-1}. Cathode: distillate water, 30 mL, 1.8 mL min^{-1}. Temperature = 80ºC.

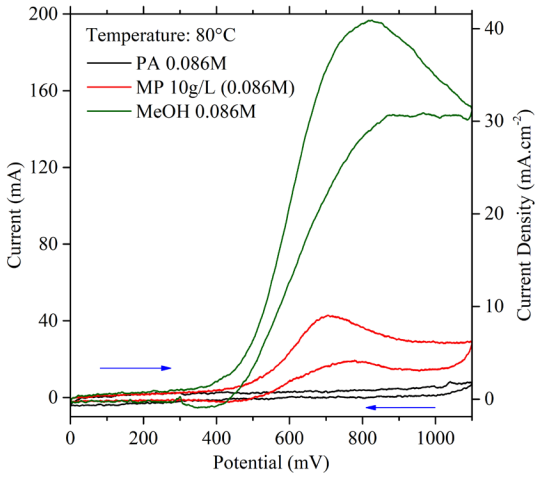

Figure 6. Comparison of electrolysis in a PEM cell of MP, methanol and pivalic acid (PA). Cyclic voltammetry (scan rate 10 mV s^{-1}) from 0 to 1100 mV (only 10^{th} cycle). Anode: MP 10 g L^{-1} in distillate water (MP electrolysis), PA 0.086 mol L^{-1} (PA electrolysis), or methanol 0.086 mol L^{-1} (MeOH electrolysis), 30 mL solution, 1.8 mL min^{-1}. Cathode: distillate water, 30 mL, 1.8 mL min^{-1}. Temperature = 80ºC.